

Experimental Demonstration of Fidelity Enhancement for Chaotic Signals in Free-Space Turbulent Channels Utilizing Vector Optical Field Manipulation

Yiqun Zhang^{1,4}, Mingfeng Xu^{2,3,4,6}, Zheng Song¹, Mengjie Zhou⁵, Jiazheng Ding⁵, Mingbo Pu^{2,3,4,6}, Kun Qiu¹, Ning Jiang^{1,*}, and Xiangang Luo^{2,3,6,*}

¹ School of Information and Communication Engineering, University of Electronic Science and Technology of China, Chengdu 611731, China

² National Key Laboratory of Optical Field Manipulation Science and Technology, Institute of Optics and Electronics, Chinese Academy of Sciences, Chengdu 610209, China

³ State Key Laboratory of Optical Technologies on Nano-Fabrication and Micro-Engineering, Institute of Optics and Electronics, Chinese Academy of Sciences, Chengdu 610209, China

⁴ Research Center on Vector Optical Fields, Institute of Optics and Electronics, Chinese Academy of Sciences, Chengdu 610209, China

⁵ Tianfu Xinglong Lake Laboratory, Chengdu 610299, China

⁶ School of Optoelectronics, University of Chinese Academy of Sciences, Beijing 100049, China

* Author e-mail address: uestc_nj@uestc.edu.cn, lxxg@ioe.ac.cn

Abstract: We experimentally demonstrate fidelity enhancement in transmitting chaotic signals through an indoor simulated kilometer-scale turbulence channel using vector optical field manipulation, which results in a 30% fidelity improvement relative to Gaussian beams under strong turbulence. © 2024 The Author(s)

1. Introduction

Enhancing the resilience of optical beam transmission in dynamically random media, such as turbulent channels, is desired for various applications, including free-space optical (FSO) communication, LIDAR, etc. Owing to time-varying inhomogeneities in refractive index and particle scattering, the quality of beams propagating in the atmosphere deteriorates, resulting in wavefront aberrations, intensity scintillation, beam divergence, and beam drift [1]. To counteract these detrimental effects, adaptive optics have been widely employed to rectify wavefront impairments in the beam effectively. However, integrating this active, real-time correction mechanism into all FSO applications poses challenges due to its intricate architecture [2].

Laser chaos is extensively employed in fiber-optic applications, including secure communication [3,4], key distribution [5], random number generation [6], and fiber-optic sensing [7], owing to its noise-like characteristics, sensitivity to initial conditions, and inherent unpredictability. Within the domain of fiber transmission, nonlinear effects serve as the primary impediments to the optimal performance of these applications, prompting a substantial body of research and various techniques designed to mitigate the influence of optical fiber nonlinearity [8]. However, it is noteworthy that there is a conspicuous absence of relevant literature addressing the phenomena and governing principles of chaotic signals transmitted through free-space turbulent channels. This absence significantly constrains the potential utilization of chaotic lasers within FSO technologies.

In this study, we utilized an indoor hot-air convective atmospheric turbulence simulation device to simulate different turbulence strengths at a distance of 1 km by adjusting the temperature difference. We conducted a comparative analysis of the transmission performance of conventional Gaussian beam, orbital angular momentum (OAM) beam, first-order cylindrical V point vector beams (radial and azimuthal), and first-order full Poincaré C point vector beams (lemon and star) after passing through the turbulent channel, focusing on center-of-mass (CofM) drift, coupled power fluctuation, and chaotic signal fidelity. The results indicate that under conditions of heightened turbulence, the transmission performance of vector beams improves over Gaussian beams, with the fidelity of chaotic signals increasing by approximately 30%.

2. Experimental setup

Figure 1 illustrates the experimental setup for transmitting laser chaotic signals through free space across a simulated turbulent channel. The chaotic signal generation is achieved using a conventional external cavity semiconductor laser (ECSL) configuration with optical feedback, which comprises a distributed-feedback laser (DFB), a polarization controller (PC), an 80:20 fiber coupler (FC1), a variable optical attenuator (VOA1), and a fiber mirror (M1). After passing through an optical isolator (ISO), the generated chaotic signal is divided into two paths via the 50:50 FC2, one of which is directed to the photodetector PD1 for detection, while the other path traverses through the erbium-doped fiber amplifier (EDFA) and the fiber collimator (COL1) before entering the vector optical field manipulation module. The generation process is detailed in the legend of Fig. 1, where the hot-air convective atmospheric turbulence simulator is positioned within the center of a 10-meter corridor. The simulator is configured with parameters that simulate a turbulent channel with a transmission distance of 1 km, a Fried

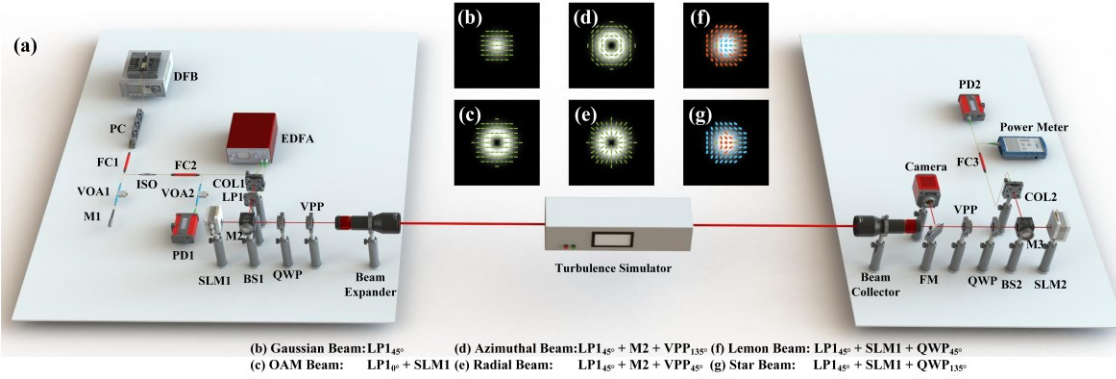


Fig. 1. (a) Experimental setup of the chaotic signal transmission system in the simulated turbulent channel. DFB, distributed-feedback laser; PC, polarization controller; FC, fiber coupler; VOA, variable optical attenuator; M, mirror; ISO, optical isolator; PD, photodetector; EDFA, erbium-doped fiber amplifier; COL, collimator; LP, linear polarizer; SLM, spatial light modulator; BS, 50-50 beam splitter; QWP, quarter-wave plate; VPP, vortex phase plate; FM, flip mirror. Intensity profile and the corresponding polarization distribution of (b) Gaussian beam; (c) OAM beam; (d) azimuthal beam; (e) radial beam; (f) lemon beam; (g) star beam.

parameter r_0 ranging from 6 to 1 (corresponding turbulence strengths expressed as D/r_0 spanning from 1 to 6). Following transmission through the turbulence channel, the beams are collected by a 10-fold beam-reduction system, which subsequently enters the vector optical field demodulation module in a symmetrical configuration with the modulation module. Afterward, the demodulated Gaussian beam is coupled into a single-mode fiber by COL2 and is then divided into two paths by a 90:10 FC3, 90% of which is detected by PD2, which calculates the cross-correlation with the data received by PD1 to assess the fidelity of the chaotic signal. The remaining portion of this path is used to monitor the coupled power fluctuation with the assistance of a highly sensitive optical power meter. On the way from the beam reduction system to the vector optical field demodulation module, an infrared camera fed by a flip mirror is employed to capture the intensity distribution of the received beam and calculate the center-of-mass drift.

3. Experimental results and Discussion

Figures 2(a)-(f) compare CofM drift in the absence of turbulence and stronger turbulence ($D/r_0 = 6$) conditions. The CofM drift serves as an indicator of beam transmission stability. It can be seen that the OAM beam experiences a large drift compared to the Gaussian beam under stronger turbulence. Conversely, all four vector beams exhibit a more stable CofM drift than the Gaussian beam, with the azimuthal vector beam demonstrating the highest level of stability, featuring a root-mean-square (RMS) value of 58.42. Fig. 2(g) illustrates the trend in RMS reduction of CofM drift for each beam concerning turbulence strength with the Gaussian beam as the reference. Under weak turbulence strength ($D/r_0 = 2$), the first-order full Poincaré beams exhibit the most effective suppression of CofM drift, achieving a reduction in RMS value of approximately 45%, and then the effectiveness of suppression for all vector beams diminishes as the turbulence strength increases. A noteworthy observation is that, under weak turbulence conditions ($D/r_0 \leq 2$), the OAM beams also exhibit some degree of drift suppression in comparison to Gaussian beams. This may be attributed to the relatively short real transmission distance of only 10 meters.

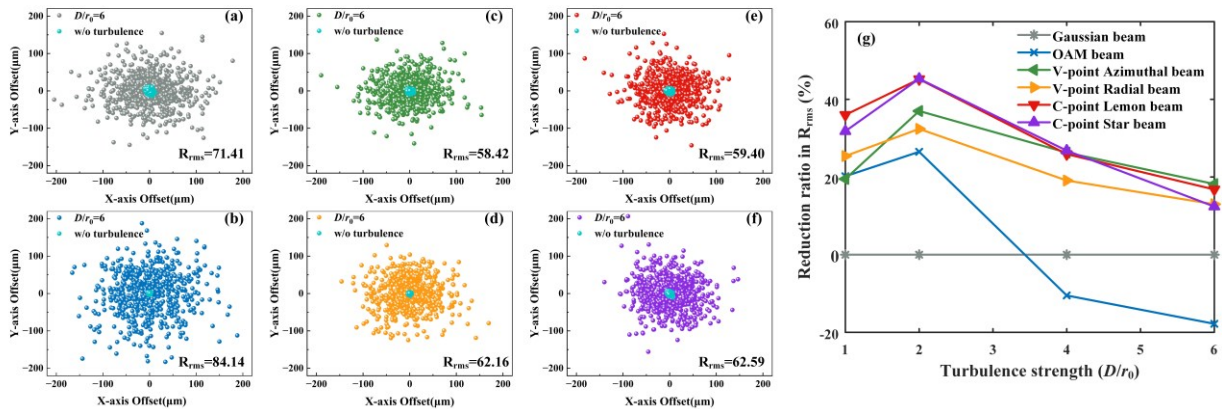


Fig. 2. (a)-(f) Statistic results of CofM variation around the optical axis of the detection system resulting from stronger turbulence with $D/r_0 = 6$ over 600 samples over 300 s for six type beams and the corresponding RMS value of the distance from samples to the center. (g) trend plot of the reduction rate in the RMS of beam CofM drift as a function of turbulence strength, with Gaussian beam as the reference.

Next, we employed the same calculation method used for spatial light intensity scintillation to investigate the power fluctuations of the six beams after demodulation and coupled at the receiving end under varying turbulence strength, since this power jitter will lead to changes in the injection strength and impacts the synchronization quality of chaotic signals. The results depicted in Fig. 3(a) demonstrated that the coupling power scintillation indexes (CPSI) for all beams increase as turbulence intensity rises, among which the Gaussian beam exhibits the most substantial CPSI, with its growth rate significantly surpassing that of the other beams, followed by the OAM beam. In contrast, the CPSIs for the four vector beams are relatively similar, highlighting their effective suppression of power fluctuation. Fig. 3(b) also displays the probability density functions (PDF) of the received optical power for the six beams under stronger turbulence. Notably, the V-point vector beams exhibit a narrower PDF and a higher bias.

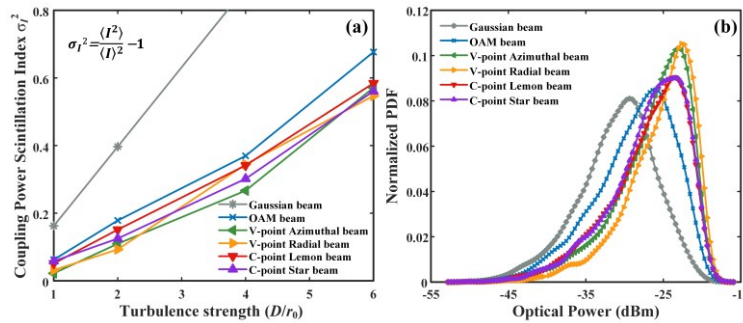


Fig. 3. (a) Coupling power scintillation index versus turbulence strength for six optical beams. (b) Probability density functions of the received optical power over 300 s of six optical beams after demodulation and coupled into a single mode fiber under stronger turbulence with $D/r_0 = 6$.

Figures 4(a)-(f) display the scatter plot depicting cross-correlation coefficients (CC) of chaotic signals at receiver and transmitter ends, continuously collected and computed under stronger turbulence strength across 50 iterations. It can be seen that the CC distribution for Gaussian and OAM beams is notably scattered, suggesting considerable instability in chaotic signals after transmission through turbulent channels. In contrast, most CC values for vector beams are concentrated at a high level. Chaotic fidelity, defined as the proportion of CC values exceeding 0.9, is employed, with 90% fidelity serving as the threshold for evaluating chaotic signal loyalty transmission characteristics. As shown in Fig. 4(g), it is evident that the chaotic fidelity of Gaussian beams rapidly decreases as turbulence strength intensifies, followed by the OAM beams. However, vector beams exhibit the capability to enhance the maximum turbulence strength tolerated by the chaotic fidelity threshold to some extent. Under stronger turbulence condition, the fidelity of the four vector beams reaches around 85%, marking an improvement of approximately 30% over the 58% fidelity of Gaussian beams. These results indicated that implementing vector optical field manipulation enhances the robustness of chaotic signal transmission in the free-space channel. This finding offers a promising avenue for further advancements in chaotic technology, particularly in the field of free-space communication, spatial key distribution, and LIDAR detection.

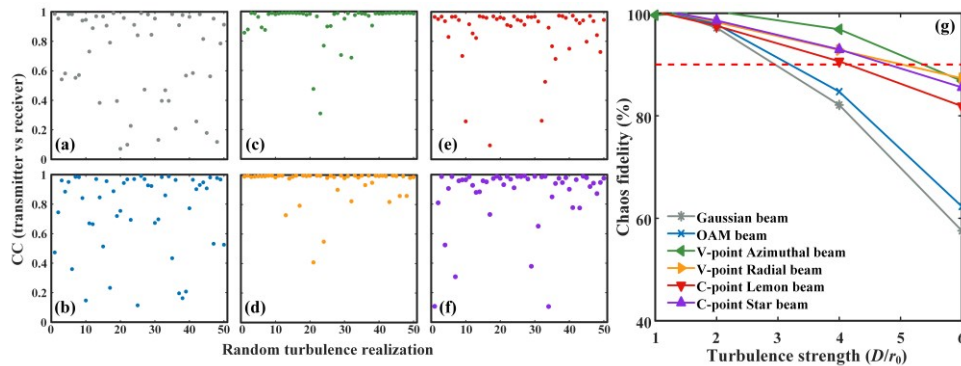


Fig. 4. (a)-(f) Measured cross-correlation coefficients between transmitter and receiver of chaotic signals over 50 emulated turbulence random realizations under stronger turbulence strength with $D/r_0 = 6$. (g) Chaos fidelity performance versus turbulence strength for six optical beams.

4. Reference

- [1] Y. Horst, et al., *Light Sci. Appl.* **12**, 153 (2023).
- [2] P. Lochab, et al., *Opt. Express* **25**, 17524-17529 (2017).
- [3] O. Spitz, et al., *Nature Commun.* **12**, 3327 (2021).
- [4] Y. Zhang, et al., *Opt. Lett.* **48**, 1470-1473 (2023).
- [5] S. Liu, et al., *Opt. Express* **30**, 32366-32380 (2022).
- [6] B. Shen, et al., *Nature Commun.* **14**, 4590 (2023).
- [7] C. Wang, et al., *Light Sci. Appl.* **12**, 213 (2023).
- [8] L. Wang, et al., *Photon. Res.* **11**, 953-960 (2023).